

# Formation Mechanism of Thermal $\text{NO}_x$ in Pulverized Coal Combustion\*

Ken OKAZAKI\*\*, Kazuo SUGIYAMA\*\* and Isao YURI\*\*

The effects of various basic factors of combustion conditions and coal properties on thermal  $\text{NO}_x$  formation behaviors in pulverized coal combustion have been experimentally clarified, and a theoretical analysis for the flame structural change around a coal particle has been performed, including full chemical kinetics of prompt  $\text{NO}_x$  formation. Thermal  $\text{NO}_x$  concentrations much higher than those predicted by the extended Zeldovich mechanism have been experimentally observed even in the usual pulverized coal combustion conditions. The contribution of thermal  $\text{NO}_x$  to the total  $\text{NO}_x$  rapidly increases with the increase of flame temperature and oxygen-fuel stoichiometric ratio, especially for highly volatile coals. Both the large amount of thermal  $\text{NO}_x$  formation and the effects of various factors on it have been well explained by considering the prompt  $\text{NO}_x$  formation in the flame zone around each coal particle through HCN and NH formed by the reactions between  $\text{N}_2$  in air and hydrocarbons in the evolved volatile matter.

**Key Words:** Combustion, Solid Fuel, Combustion Products, Furnace, Chemical Reaction, Fossil-Fuel-Fired Power Generation, Pulverized Coal Combustion,  $\text{NO}_x$  Formation, Thermal  $\text{NO}_x$

## 1. Introduction

Nitric oxides ( $\text{NO}_x$ ) can be formed, in general, from oxidation of nitrogen compounds in the fuel (fuel  $\text{NO}_x$ ) and the fixation of atmospheric nitrogen (thermal  $\text{NO}_x$ ), but fuel  $\text{NO}_x$  is considered to be the major contribution to the total  $\text{NO}_x$  for the usual burning conditions of pulverized coal<sup>(1),(2)</sup>. This is the reason why most of the recent studies on  $\text{NO}_x$  in pulverized coal combustion<sup>(9)-(10)</sup> have been devoted to identifying the mechanism of conversion processes from coal-N (volatile-N and char-N) to  $\text{NO}_x$  and why most theoretical studies<sup>(11),(12)</sup> have neglected the formation of thermal  $\text{NO}_x$ . These continuing energetic studies have revealed the important features of  $\text{NO}_x$  formation and the method of suppressing it by staging or controlling the local burning conditions in the furnace. Actually, the technologies to simultaneously reduce in-furnance  $\text{NO}_x$  concentration to less than 150 ppm and unburnt carbon in ashes to less than 5 wt% have already been achieved in Japan<sup>(13)</sup>.

Such progress in low- $\text{NO}_x$  combustion technology has changed the situation, resulting in the increase of the relative importance of thermal  $\text{NO}_x$  contribution

even in pulverized coal combustion. However, thermal  $\text{NO}_x$  formation behavior in pulverized coal combustion and its mechanisms have not been investigated in detail.

The purpose of this study is to clarify the fundamental and general features of thermal  $\text{NO}_x$  formation characteristics in pulverized coal combustion through experiments and theoretical analyses. First, the pure effects of various important factors of the oxygen-fuel stoichiometric ratio, initial oxygen concentration, maximum flame temperature, and coal properties of volatile matter and nitrogen content are experimentally investigated. Then, the mechanisms of these effects are clarified by theoretical analyses which include full chemical kinetics of prompt  $\text{NO}_x$  formation in the flame zone around each coal particle. Although the term "prompt  $\text{NO}_x$ " is generally used for the  $\text{NO}_x$  rapidly formed in the premixed fuel-rich hydrocarbon flame<sup>(14)</sup>, here we use it for the  $\text{NO}_x$  formed in the flame zone around coal particles through the intermediate species of HCN and NH, from the reactions of  $\text{N}_2$  in air with hydrocarbons evolved from coal particles as volatile matter.

## 2. Experimental System and Procedure

The one-dimensional combustion furnace used in the experiments and its flow system are almost the same as our previous one<sup>(9),(15)</sup> but it has been recon-

\* Received 11th June, 1991. Paper No. 89-1448A

\*\* Department of Energy Engineering, Toyohashi University of Technology, Tempaku-cho, Toyohashi, Aichi 441, Japan

structured so as to suit our present study. The furnace is 1.5 m in length, 8 cm in inner diameter and constructed with water-cooled steel cylinders with heat-insulating refractory coated on the inside. Moreover, argon gas lines have been newly attached to supply a nitrogen-free Ar/O<sub>2</sub> mixture. An air preheating system and O<sub>2</sub> injector have also been installed to independently control the flame temperature and initial oxygen concentration. The gaseous samples were analyzed by using standard continuous instruments of chemiluminescent NO<sub>x</sub>, paramagnetic O<sub>2</sub>, NDIR CO/CO<sub>2</sub> and FID total hydrocarbon to monitor the combustion.

Ultimate and proximate analyses of the three kinds of coals, A, B and C, used in this study are shown in Table 1. Coals A and B are lignite and sub-bituminous and have almost the same volatile matter content (VM) but much different nitrogen content (N). On the other hand, bituminous coal C has much lower volatile matter content than those of A and B but almost the same high content of fuel nitrogen as that of coal B.

Experiments are performed for widely varied experimental parameters of the oxygen-fuel stoichiometric ratio  $\lambda$  (0.8–1.4), initial oxygen concentration  $R_{O_2}$  (21–27 vol%) and maximum flame temperature  $T_{max}$  (1 100–1 600°C). In order to derive the pure effects of these various experimental parameters, CR values, defined as the ratio of measured NO<sub>x</sub> concentration to that of 100% conversion from fuel-N under the same given experimental condition, are mostly used in the data reductions not only for fuel NO<sub>x</sub> but also for thermal NO<sub>x</sub> and total-NO<sub>x</sub> in this study. According to the fact that interactions between fuel NO<sub>x</sub> and thermal NO<sub>x</sub> are not of first-order importance<sup>(1)</sup>, thermal NO<sub>x</sub> can be specified by subtracting fuel NO<sub>x</sub> obtained by use of Ar+O<sub>2</sub> as an oxidant from total NO<sub>x</sub> by N<sub>2</sub>+O<sub>2</sub> at a given condition with the relevant basic factors being perfectly matched.

### 3. Experimental Results and Discussion

The concentration profiles of total NO<sub>x</sub> and fuel NO<sub>x</sub> have their maximum values near the position of maximum flame temperature and then decrease gradually. Therefore,  $T_{max}$  was selected as one of the basic combustion parameters affecting NO<sub>x</sub> formation. In the following, the final NO<sub>x</sub> concentrations measured

Table 1 Coal properties

Coal	Proximate Analysis(% dry)			Ultimate Analysis(% dry)					
	VM	FC	Ash	C	H	O	N	S	
A	44.4	39.8	15.8	65.4	5.47	12.5	0.79	0.21	
B	40.8	49.2	10.0	71.4	5.3	10.9	1.50	0.74	
C	26.1	58.7	15.2	70.5	3.64	8.3	1.64	0.99	

VM : Volatile Matter, FC : Fixed Carbon

at the exit of the furnace are used to discuss the NO<sub>x</sub> formation characteristics.

#### 3.1 Effect of flame temperature

Temperature dependence of the formation characteristics of thermal NO<sub>x</sub> and fuel NO<sub>x</sub> for highly volatile coal A and its changes with the increase of oxygen-fuel stoichiometric ratio  $\lambda$  are shown in Fig. 1, where measured NO<sub>x</sub> concentrations are converted to CR values defined above. On the whole, the CR values for total NO<sub>x</sub> increase with the increase of maximum flame temperature  $T_{max}$  due to the increase of thermal NO<sub>x</sub> formation, while the fuel NO<sub>x</sub> is insensitive to the flame temperature. A temperature dependence of fuel NO<sub>x</sub>, which might be evident for very high temperatures<sup>(1),(9)</sup>, has not been observed in the temperature range tested in this study. For the temperatures below 1 200°C, thermal NO<sub>x</sub> contributions in the total NO<sub>x</sub> disappear. It is interesting that the CR values for total NO<sub>x</sub> and fuel NO<sub>x</sub> are almost on the same line, respectively, in spite of the different initial oxygen concentrations. This is consistent with our previous report<sup>(15)</sup> that oxygen concentration itself has little effect on NO<sub>x</sub> formation if the maximum flame temperature is fixed. Although a higher oxygen concentration elevates the particle temperature and promotes the evolution of volatile matter, its effect may have been compensated by the contraction of the flame zone around coal particles where prompt NO<sub>x</sub> is mainly formed, as will be discussed in the theoretical analysis.

It is also shown in Fig. 1 that the temperature dependency of thermal NO<sub>x</sub> increases with the increase of the oxygen-fuel stoichiometric ratio  $\lambda$ . For the flame temperature of 1400°C, the contribution of thermal NO<sub>x</sub> to the total NO<sub>x</sub> is 15% for  $\lambda=0.8$  and 1.0, 22% for  $\lambda=1.2$ , and 33% for  $\lambda=1.4$ . Although the result for  $\lambda=1.2$  is almost the same as that of Pershing and Wendt<sup>(1)</sup>, much larger amounts of thermal NO<sub>x</sub> are formed for larger values of  $\lambda$  if the temperature is fixed.

The results shown in Fig. 1 should change depending on the coal properties. Figure 2 shows such effects with the oxygen-fuel stoichiometric ratio fixed at 1.2. Temperature dependence of thermal NO<sub>x</sub> decreases with the decrease of volatile matter in coal. At the temperature of 1 400°C, while the contribution of thermal NO<sub>x</sub> to the total NO<sub>x</sub> is 22% for highly volatile coals A and B, it decreases to 15% for low-volatility coal C. In the latter case, the CR values for both thermal NO<sub>x</sub> ( $CR_{th}$ ) and fuel NO<sub>x</sub> ( $CR_f$ ) are much lower than those for coals A and B. The large values of both  $CR_{th}$  and  $CR_f$  for coal A are due to the low nitrogen content of coal A<sup>(15)</sup>.

### 3.2 Effect of oxygen-fuel stoichiometric ratio

From raw data such as those shown in Fig. 1, the pure effects of the oxygen-fuel stoichiometric ratio  $\lambda$

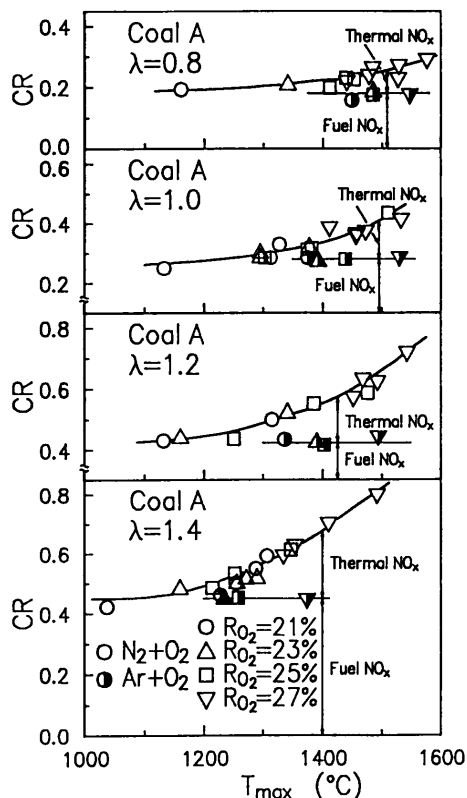


Fig. 1 Temperature dependence of thermal  $\text{NO}_x$  formation characteristics for coal A and its changes with oxygen-fuel stoichiometric ratio

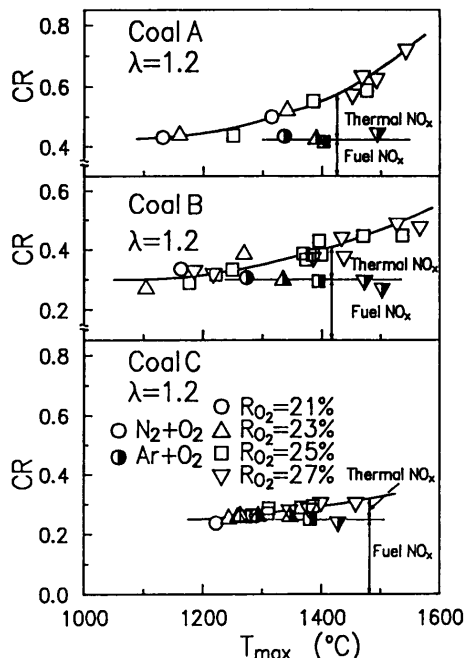


Fig. 2 Temperature dependence of thermal  $\text{NO}_x$  formation characteristics for a fixed oxygen-fuel stoichiometric ratio of 1.2 and its changes by coal types

can be derived by determining the  $CR$  values for various fixed values of flame temperature. The results thus obtained for coals A, B and C are shown in Fig. 3 for the maximum flame temperatures of 1 300, 1 400 and 1 500°C. As for the thermal  $\text{NO}_x$ , not only the values of  $CR_{th}$  but also the concentrations of thermal  $\text{NO}_x$  reduced to those at the standard condition of  $R_{O_2} = 21 \text{ vol\%}$  and  $\lambda = 1.0$  are also shown in the lower figures.

It is shown that the dependence of thermal  $\text{NO}_x$  on the oxygen-fuel stoichiometric ratio  $\lambda$  is much larger than that of fuel  $\text{NO}_x$ , although both thermal  $\text{NO}_x$  and fuel  $\text{NO}_x$  increase with increase of  $\lambda$ . Thermal  $\text{NO}_x$  monotonously increases with  $\lambda$ , while fuel  $\text{NO}_x$  shows a tendency to saturate<sup>(16)</sup> for  $\lambda > 1.2$ . Moreover, the increase of thermal  $\text{NO}_x$  with  $\lambda$  is much more significant for higher temperatures. In the case of a high temperature of 1 500°C for coal A, 33% and 42% of the total  $\text{NO}_x$  are due to thermal  $\text{NO}_x$  for  $\lambda = 1.2$  and 1.4, respectively. On the other hand, only a small contribution of thermal  $\text{NO}_x$  can be observed for the case of the low temperature of 1 300°C, where only 10% of the total  $\text{NO}_x$  is due to thermal  $\text{NO}_x$  even for the fuel-lean condition of  $\lambda = 1.2$ .

Figures 1, 2 and 3 show the strong effect of flame temperature in increasing the thermal  $\text{NO}_x$  formation.

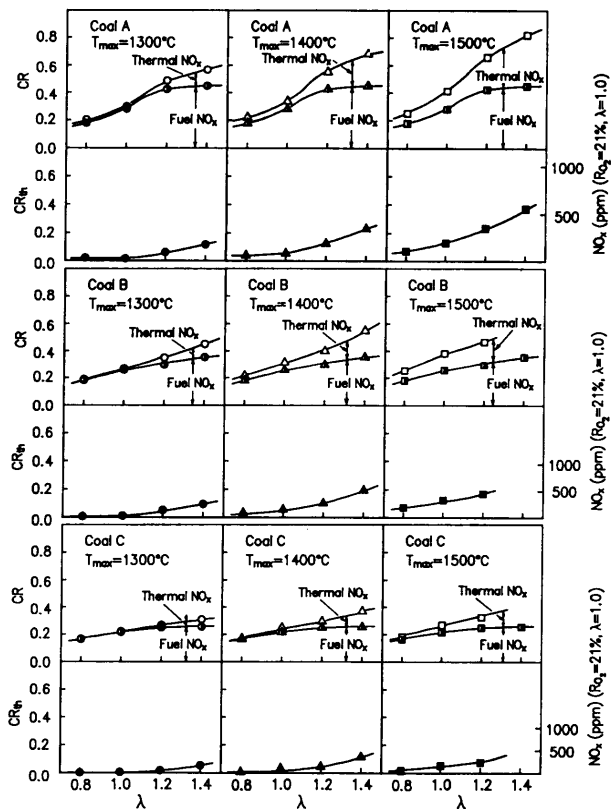


Fig. 3 Effect of oxygen-fuel stoichiometric ratio on thermal  $\text{NO}_x$  and fuel  $\text{NO}_x$  formation characteristics. The maximum flame temperatures are fixed at 1 300, 1 400 and 1 500°C

Here, the concentrations of Zeldovich  $\text{NO}_x$  formed by the well-known extended Zeldovich mechanism (Eqs. (10), (11) and (12) in section 4.2) were estimated. Because the volatile matter burns in a very short time and the Zeldovich  $\text{NO}_x$  is mainly formed in the post-flame, the increasing behavior of Zeldovich  $\text{NO}_x$  concentration was calculated with the oxygen concentration after the volatile matter combustion as the initial condition. The results obtained for the case of  $\lambda=1.2$  and coal A are shown in Fig. 4. The broken line shows the residence time corresponding to the actual experiments.

According to this estimation, the Zeldovich  $\text{NO}_x$  concentration is only 1 ppm at the fixed temperature ( $T$ ) of 1 800 K and 40 ppm at  $T=2\ 000$  K, and is much smaller than the thermal  $\text{NO}_x$  concentrations shown in Fig. 3. The large discrepancy cannot be explained even if we consider the fact that the actual particle temperature can be much higher than the flame temperature<sup>(17),(18)</sup>, especially in the region of volatile matter combustion.

In this paper, the prompt  $\text{NO}_x$  formed in the flame zone around coal particles during volatile matter combustion is considered to be the major source of the thermal  $\text{NO}_x$ , as shown in the theoretical analysis below. In pulverized coal combustion, the increase of temperature will expand for flame zone further away from the surface of coal particles, which results in the increase of prompt  $\text{NO}_x$  formation in it, while the prompt  $\text{NO}_x$  formation itself is usually affected very little by the temperature.

### 3.3 Effect of coal properties

Comparing the results for coals B and C having almost the same nitrogen content, the separate effect of volatile matter content on the thermal  $\text{NO}_x$  formation was derived. Larger values of volatile matter content result in the increase of thermal  $\text{NO}_x$ , and this

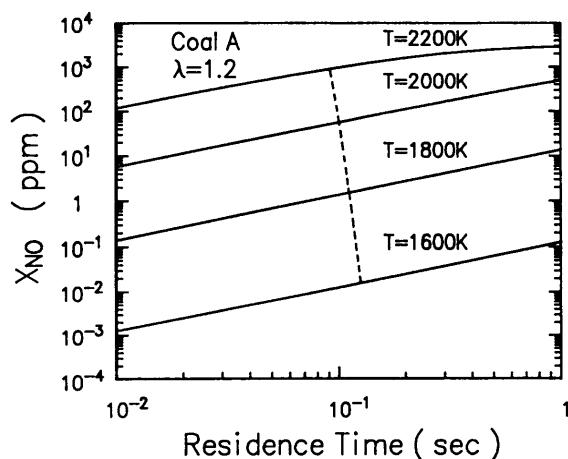


Fig. 4 Estimation of thermal  $\text{NO}_x$  formation only by the extended Zeldovich mechanism for coal A and oxygen-fuel stoichiometric ratio of 1.2

effect is larger for higher values of  $T_{\max}$  and  $\lambda$ . This effect can be explained as that the higher volatile matter content will result in the greater expansion of the hot flame zone around burning particles<sup>(17),(19),(20)</sup>, where the prompt  $\text{NO}_x$  can easily be formed<sup>(10)</sup>.

The separate effect of nitrogen content on the thermal  $\text{NO}_x$  formation can be derived by comparing the results for coals A and B having almost the same high volatile matter content. As a result, the effect of fuel nitrogen content on the thermal  $\text{NO}_x$  formation is quite small, and no significant effect has been observed.

## 4. Theoretical Analysis of Thermal $\text{NO}_x$ Formation

Combining the full chemical kinetics scheme for laminar diffusion flames of methane<sup>(21)</sup> with our model for the time-dependent changes of flame structure around a coal particle<sup>(17)</sup>, thermal  $\text{NO}_x$  formation behavior around a coal particle was theoretically analyzed. The purpose of this analysis is to show how a large amount of prompt  $\text{NO}_x$  can be formed near the particles, and is not to establish a strict model for predicting  $\text{NO}_x$  concentrations nor to discuss detailed chemical kinetics. Hence, the most simplified model fitting the present purpose is adopted in this study.

### 4.1 Analytical model

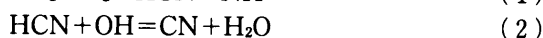
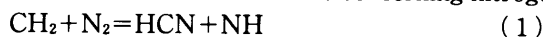
The following assumptions are introduced in the analysis.

- (1) A coal particle is spherical and all phenomena considered are spherically symmetric.
- (2) Only methane ( $\text{CH}_4$ ) is considered as evolved volatile matter.
- (3) Fixed carbon is oxidized on the particle surface by  $\text{O}_2$  and  $\text{CO}_2$ .
- (4) Particle diameter is constant during the volatile matter combustion.
- (5) Radial velocity is calculated from the evolving flux of volatile matter and combustion products; then the momentum conservation equation is excluded.
- (6) Gas and particle temperatures are the same and constant at the given value; then the energy conservation equation is excluded.

Based on the above assumptions, the fundamental equations consist of conservation equations of mass and species in the gas phase and mass of the solid phase. As for boundary conditions for the species concentrations, their gradients at the outer radius of the equivalent sphere occupied by one coal particle are given as zero. Raw coal and surrounding air are simultaneously set at the given temperature at the time  $t=0$ . Then, time-dependent changes of chemical structures in the flame around the particle are calculated.

## 4.2 Gas phase reaction model

Fuel  $\text{NO}_x$  is not considered in this model and only thermal  $\text{NO}_x$  formation behaviors are analyzed. In the analysis here,  $\text{NO}_x$  is treated as  $\text{NO}$ . The following 12 reactions are considered as those concerning nitrogen.



The fragment of  $\text{CH}_4$  reacts with  $\text{N}_2$  in air to produce  $\text{HCN}$  and  $\text{NH}$  (reaction (1)), which then react with  $\text{OH}$  to yield  $\text{CN}$  and  $\text{N}$  (reactions (2) and (5)). Through the oxidation of those intermediate species, the prompt  $\text{NO}$  is formed in the flame zone around a coal particle. Reactions (10), (11) and (12) correspond to the extended Zeldovich mechanism and form Zeldovich  $\text{NO}$ . Numerical calculations have been performed considering 20 chemical species and 44 elemental reactions, whose kinetics data were evaluated by citing the references<sup>(21),(22)</sup>. Zeldovich  $\text{NO}$  can be separately specified by stopping reaction (1).

## 4.3 Analytical results and discussion

Figures 5 and 6 show the time-dependent concentration profiles of chemical species around a particle of coal A with a diameter of  $70 \mu\text{m}$  immersed in the constant temperature field of  $1700 \text{ K}$  and  $R_{\text{O}_2} = 21 \text{ vol\%}$ .  $\text{HC}$  in Fig. 5 is the sum of  $\text{CH}_4$ ,  $\text{CH}_3$  and  $\text{CH}_2$ . In the stage of volatile matter combustion, the flame zone, whose position is defined as that of the intersec-

tion of  $\text{HC}$  and  $\text{O}_2$ , is pushed away from the particle surface in a very short time by the evolution of volatile matter and then shrinks back to the particle surface with the consumption of volatile matter. The times shown in these figures are rather short because the preheating time is not taken into account. It is shown in Fig. 6 that large amounts of  $\text{HCN}$  and  $\text{NH}$  are actually formed in the fuel-rich zone inside the flame, resulting in  $\text{NO}$  formation slightly outside the flame. The  $\text{NO}$  formed in the flame zone will diffuse to the outer region with the progress of time.

Comparison between thermal  $\text{NO}$  and Zeldovich  $\text{NO}$  concentration profiles around a particle at the time  $t = 5 \text{ ms}$  is shown in Fig. 7. Zeldovich  $\text{NO}$  gives only a small contribution to the thermal  $\text{NO}$ , and the rest is due to the prompt  $\text{NO}$ . Here, it has been clarified for the first time that the thermal  $\text{NO}$  formation in pulverized coal combustion is mostly due to the prompt  $\text{NO}$  formed in the flame zone around coal particles.

The  $\text{NO}$  concentration profiles thus obtained at each time have been averaged in space, and the changes of thermal  $\text{NO}$  and Zeldovich  $\text{NO}$  concentrations with elapsed time have been obtained as shown in Fig. 8, including the effect of temperature. Average concentrations of thermal  $\text{NO}$  rapidly increase in the stage of volatile matter combustion and subsequently saturate. These results are quite reasonable because the thermal  $\text{NO}$  is mainly due to the prompt  $\text{NO}$  formed in the flame zone around coal particles during the volatile matter combustion. Now, the large discrepancy between the measured thermal  $\text{NO}_x$  concentration and that of estimated Zeldovich  $\text{NO}_x$ , as mentioned in the previous section 3.2, has been very well explained by considering the prompt  $\text{NO}_x$  formation. Although the actual combustion behavior of coal particles in pulverized coal combustion<sup>(20),(23)</sup> is not so

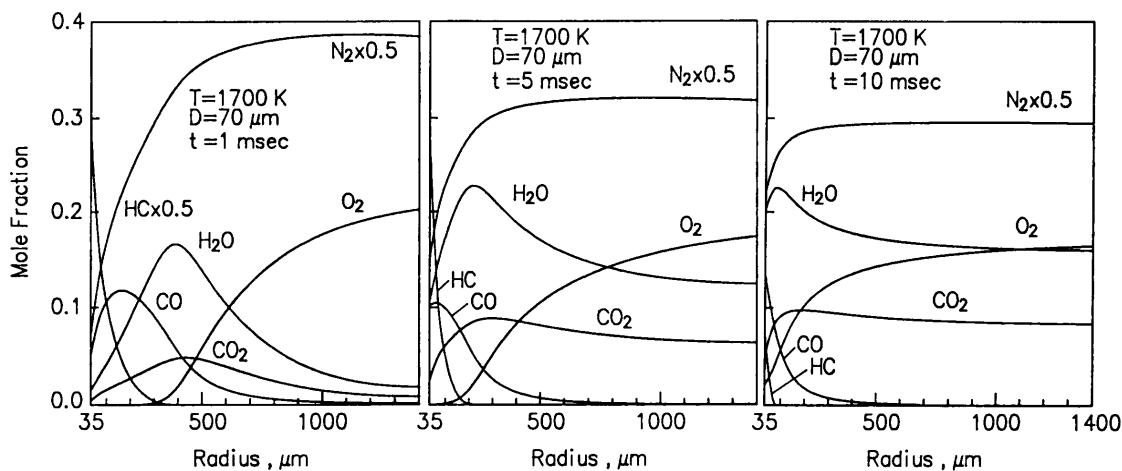


Fig. 5 Time-dependent concentration profiles of major stable chemical species in the flame around a coal A particle of  $70 \mu\text{m}$  in diameter at the temperature of  $1700 \text{ K}$

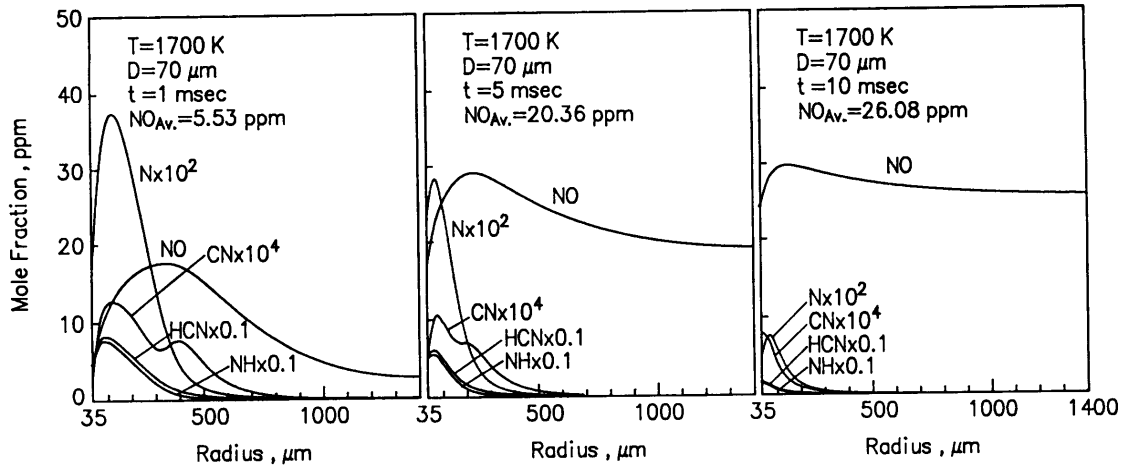


Fig. 6 Time-dependent concentration profiles of nitrogen-containing chemical species in the flame around a coal A particle of 70  $\mu\text{m}$  in diameter at the temperature of 1700 K

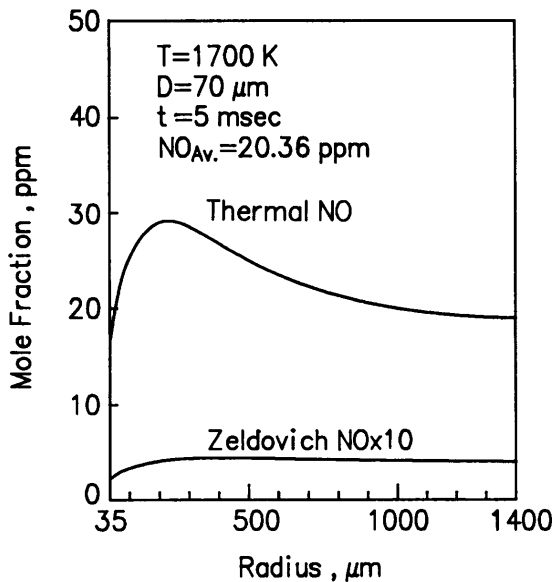


Fig. 7 Comparison of the concentrations and their profiles of thermal NO and Zeldovich NO around a coal A particle of 70  $\mu\text{m}$  in diameter at  $T=1700\text{ K}$  and  $t=5\text{ ms}$

simple as the model adopted in this analysis, it should be true that the thermal  $\text{NO}_x$  is mainly due to the prompt  $\text{NO}_x$ .

The very slight effect of initial oxygen concentration ( $R_{O_2}$ ) on the thermal  $\text{NO}_x$  formation, as discussed in the experiments, can also be well explained by this analysis which includes prompt  $\text{NO}_x$  formation, as shown in Fig. 9. The radius of the flame center at  $t=1\text{ ms}$  decreased from 310  $\mu\text{m}$  for  $R_{O_2}=21\text{ vol}\%$  to 260  $\mu\text{m}$  for  $R_{O_2}=27\text{ vol}\%$ , and this shrinkage of the flame zone cancelled the pure effect of oxygen concentration on the thermal  $\text{NO}_x$  formation.

### 5. Conclusions

Thermal  $\text{NO}_x$  formation characteristics in pulver-

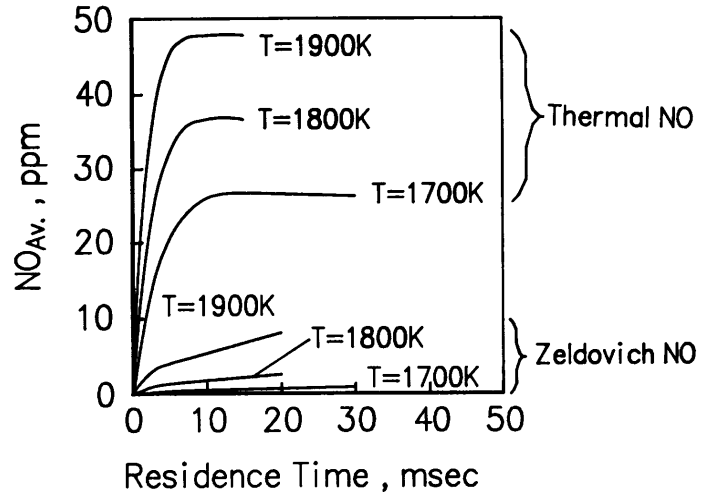


Fig. 8 Increasing behavior of average concentrations of thermal NO and Zeldovich NO with elapsed time and the dependencies on temperature for a 70- $\mu\text{m}$  particle of coal A

ized coal combustion have been investigated both experimentally and theoretically, and the following conclusions have been derived.

1) A much larger amount of thermal  $\text{NO}_x$  can be formed than that predicted by the extended Zeldovich mechanism for the maximum flame temperature. This is mainly due to the prompt  $\text{NO}_x$  formation in the flame zone around coal particles during volatile matter combustion.

2) Thermal  $\text{NO}_x$  contribution to the total  $\text{NO}_x$  rapidly increases with the increase of maximum flame temperature, and this tendency is much stronger for higher values of oxygen-fuel stoichiometric ratio and volatile matter content.

3) Initial oxygen concentration does not have such a significant effect on the thermal  $\text{NO}_x$  formation under the same maximum flame temperature. This is due to the fact that the shrinkage of the expanding

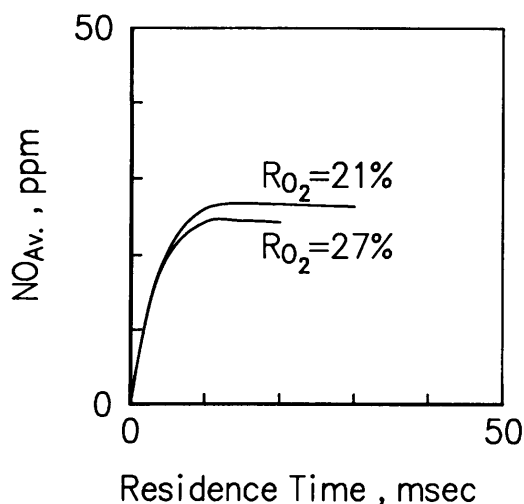


Fig. 9 Effect of initial oxygen concentration in the oxidant on the formation behavior of thermal NO for a 70- $\mu\text{m}$  particle of coal A

flame zone around coal particles negates the pure effect of the increase of oxygen concentration.

4) Thermal  $\text{NO}_x$  formation monotonously increases with the increase of the oxygen-fuel stoichiometric ratio, while the fuel  $\text{NO}_x$  formation tends to saturate at an oxygen-fuel stoichiometric ratio larger than 1.2. The former tendency is more significant for higher flame temperature and higher volatile matter content.

5) Coals of higher volatile matter content result in the increase of thermal  $\text{NO}_x$  formation especially for the case of high temperature and large oxygen-fuel stoichiometric ratio. This is due to the expansion of the flame zone around coal particles where the prompt  $\text{NO}_x$  is easily formed.

### References

- (1) Pershing, D. W. and Wendt, J. O. L., Sixteenth Symposium (International) on Combustion, The Combustion Institute, (1977), p. 389.
- (2) Pershing, D. W. and Wendt, J. O. L., I & EC Process Design and Development, Vol. 18, No. 1 (1979), p. 60.
- (3) Pohl, J. H. and Sarofim, A. F., Sixteenth Symposium (International) on Combustion, The Combustion Institute, (1977), p. 491.
- (4) Wendt, J. O. L., Pershing, D. W., Lee, J. W. and Glass, J. W., Seventeenth Symposium (International) on Combustion, The Combustion Institute, (1979), p. 77.
- (5) Altenkirch, R. A., Peck, R. E. and Chen, S. L., Combust. Sci. Technol., Vol. 20 (1979), p. 49.
- (6) Song, Y. H., Pohl, J. H., Beer, J. M. and Sarofim, A. F., Combust. Sci. Technol., Vol. 28 (1982), p. 31.
- (7) Chen, S. L., Heap, M. P., Pershing, D. W. and Martin, G. B., Nineteenth Symposium (International) on Combustion, The Combustion Institute, (1982), p. 1271.
- (8) Peck, R. E., Midkiff, K. C. and Altenkirch, R. A., Twentieth Symposium (International) on Combustion, The Combustion Institute, (1984), p. 1373.
- (9) Okazaki, K., Shishido, H., Nishikawa, T. and Ohtake, K., Twentieth Symposium (International) on Combustion, The Combustion Institute, (1984), p. 1381.
- (10) Phong-Anant, D., Wibberley, L. J. and Wall, T. F., Combust. Flame, Vol. 62 (1985), p. 21.
- (11) Smith, P. J., Hill, S. C. and Smoot, L. D., Nineteenth Symposium (International) on Combustion, The Combustion Institute, (1982), p. 1263.
- (12) Hill, S. C., Smoot, L. D. and Smith, P. J., Twentieth Symposium (International) on Combustion, The Combustion Institute, (1984), p. 1391.
- (13) Ohtake, K., Present Status and Future Aspects of Science and Technology on Pulverized Coal Combustion in Japan. Paper presented at the Western States Section Meeting, The Combustion Institute, Tucson, Arizona, Oct. (1986).
- (14) Fenimore, C. P., Thirteenth Symposium (International) on Combustion, The Combustion Institute, (1971), p. 373.
- (15) Okazaki, K., Ohya, M., Yuri, I. and Ohtaka, K., Coal Combustion: Science and Technology of Industrial and Utility Applications (Ed. J. Feng), Hemisphere, (1988), p. 821.
- (16) Takagi, T., Tatsumi, T. and Ogasawara, M., Combust. Flame, Vol. 35 (1979), p. 17.
- (17) Takeshi, M. and Okazaki, K., Temperature History of Burning Particles with Scattering, Absorbing and Emitting in Pulverized Coal Combustion, Paper presented at the first International Symposium on Coal Combustion, Beijing, China, Sept. (1987).
- (18) Saitoh, M., Sadakata, M., Sato, M. and Sakai, T., Bull. Chemical Engineering, Japan, (in Japanese), Vol. 13, No. 4 (1987), p. 451.
- (19) Mclean, W. J., Hardesty, D. R. and Pohl, J. H., Eighteenth Symposium (International) on Combustion, The Combustion Institute, (1981), p. 1239.
- (20) Seeker, W. R., Samuelsen, G. S., Heap, M. P. and Trolinger, J. D., Eighteenth Symposium (International) on Combustion, The Combustion Institute, (1981), p. 1213.
- (21) Mori, Y., Miyauchi, T., Inoue, H. and Ohtake, K., Trans. Jpn. Soc. Mech. Eng., (in Japanese), Vol. 46, No. 410, B (1980), p. 2052.
- (22) Westbrook, C. K. and Chase, L. L., Chemical Kinetics and Thermochemical Data for Combustion Applications, Lawrence Livermore Lab., Univ. of Calif., (1982).
- (23) Beer, J. M., Coal Combustion: Science and Technology of Industrial and Utility Applications (Ed. J. Feng), Hemisphere, (1988), p. 1.